FSS 000232 R

MEASUREMENTS OF GAS VELOCITIES AND TEMPERATURES IN A LARGE OPEN POOL FIRE

M. E. Schneider and L. A. Kent
Thermal Test and Analysis Division
Sandia National Laboratories
Albuquerque, New Mexico

ABSTRACT

There is an interest in determining the response and survivability of a variety of items subject to engulfment in a large fire which may occur in a transportation accident. In order to estimate this response, knowledge of the thermal and flow conditions prevailing in these pool fires is required. Few experiments have been performed with large (>3 meter diameter) fires. In particular, velocity measurements in the continuous flame region of low Froude number fires are very scarce. Scaling up the results of small pool fires is problematic due to the large number of relevant dimensionless variables to be matched.

A total of ~ 48,500 liters of JP-4 fuel was burned in a 9x18 meter pool, producing peak temperatures in excess of 1230 °C (2250 °F), over much of the instrumented region of the flame. Temperatures were measured at 28 locations throughout the continuous flame region with 1.587 mm OD Inconel sheathed, ungrounded, type K thermocouples. Four 0.127 mm diameter bare wire thermocouples were used to make high frequency response temperature measurements. Velocities were measured at four vertical stations near the centerline of the pool, with glass coated, velocity probes. Heat fluxes were estimated from measurements on and near vertically suspended mild steel plates.

As is often the case in fires of this size, the effects of mild ambient winds on the measurements were pronounced. Attempts have been made to mitigate these effects by the application of conditional sampling. Temperatures are compared with measurements made in other large aviation fuel fires. The measured velocities are slightly less than would be predicted from an empirical model that was developed from experimental results for methane diffusion flames that are orders of magnitude smaller.

This test program was funded by the Department of Energy (DOE) and was directed by the Transportation Technology Center at Sandia National Laboratories. Sandia National Laboratories is operated by AT&T Technologies for the U.S. Department of Energy (DOE) under Contract DE-AC04-76DP00789

NOMENCLATURE

A	-	Pool surface area [m^2]
C	-	Calibration constant (near 1.00)
$C_{p,\infty}$	-	Specific heat of ambient air [J/kg °K]
D	-	Pool Diameter [m]
Fr_o	-	Froude number, W_o^2 / gD
g	-	Acceleration of gravity [m/s^2]
h	-	Convective heat transfer coefficient [W/m^2 °K]
$\dot{Q}$	-	Heat release rate [kW]
Q_c	-	Convective heat release rate [kW]
Q^*	-	Dimensionless heat release rate
Re_D	-	Reynolds number based on probe diameter
T_f	-	Flame temperature [°K]
T_s	-	Surface temperature [°K]
T_∞	-	Ambient temperature [°K]
W	-	Upward gas velocity [m/s]
W_o	-	Initial upward velocity [m/s]
z	-	Vertical distance [m]
z'	-	Scaled vertical distance
ΔP	-	Pressure difference [N/m^2]
ϵ	-	Emissivity
σ	-	Boltzmann constant [W/m^2 °K^4]
ρ	-	Gas density [kg/m^3]
ρ_∞	-	Ambient air density [kg/m^3]

INTRODUCTION & LITERATURE REVIEW

In order to estimate the response of items in fires resulting from transportation accidents, an understanding of the flow field and temperature distribution in such fires is crucial. Fires resulting from transportation accidents are most often due to the spillage and ignition of hydrocarbon fuels. There is interest in improving the understanding of large turbulent fires resulting from such spills.

It is quite difficult and expensive to perform experiments at full scale; the question of scaling must therefore be addressed. It would be desirable to perform tests with smaller fires, if the results can be scaled up to the sizes of typical accidental fires. Much work has been done investigating the problem of scaling fires. A number of considerations are pertinent when comparing fires:

- Is the fire's flowfield dominated by buoyancy or momentum forces ?
- Is the burning rate determined by radiation or convection of the flame's heat back to the pool surface ?
- What fraction of the radiation from the flame region escapes to the ambient ?
- Is the flow laminar or turbulent ?

The question of buoyancy vs. momentum domination will be addressed first. The available literature indicates that a number of different flow regimes are possible. If the velocity of fuel vapor is high at the pool surface, or if a jet of gaseous fuel is being burned, the initial jet momentum will control the fluid mechanics. As the jet velocity is lowered the transition between momentum dominated flow and buoyancy dominated flow starts above the flame tip and moves down toward the burning surface, or jet exit. At very low exit velocities, the flow is buoyancy dominated from the start. This buoyancy domination is commonly the case with pool fires, due to the low initial velocities near the pool surface. The entrainment rate of ambient air into the fire plume is quite different for buoyancy controlled flames than for momentum dominated flames. The exit velocity to buoyancy ratio is related to the heat release per unit area. Zukoski [1], defines a dimensionless heat release, Q^*, which can be used to determine the expected behavior of a buoyant fire. The definition is :

$$Q^* = \frac{\dot{Q}}{\rho_\infty C_{p\infty} T_\infty \sqrt{gD}\, D^2} \qquad (1)$$

Other studies have used the Froude number to perform similar analyses. The Froude number is based on the initial velocity, W_o, and is given by : $Fr_o = W_o^2/gD$. It should be noted that Q^* is proportional to the square root of the Froude number. The flow can be divided into three flame regimes. The flame may be totally dominated by momentum, it may switch from momentum domination to buoyancy domination at some height, or it may be totally buoyancy driven. Zukoski splits the buoyancy driven flames into two regimes, one where the flame height is a function of fire diameter, and one in which individual flamelets of fixed height determine the total flame height independent of pool size. The buoyancy starts to play some role near the upper portion of the flame for $Q^* \approx 10000$. When $Q^* \approx 100$ the buoyancy has influence even at the pool surface, (burner exit). A transition is observed at $Q^* \approx 0.3$ at which the flame breaks up into individual flamelets. It is expected that at this point it becomes very difficult for oxygen to be entrained to the pool center. Typical values of Q^* for large fuel spill fires range from 0.6 to 1.0. In scaling down the large open pool hydrocarbon fire, it is necessary to insure that Q^* is less than 1.

In buoyant diffusion flames with Q^* near 1, McCaffrey [2] has defined 3 fire zones based on the vertical distance scaled by the heat release rate. The scaling is meant to allow data at various heights from fires of different fuels to be compared. The scaled distance is given by : $z' = z/Q^{2/5}$. The region $z' < 0.08$ is referred to as the continuous flame region. The intermittent flame region is $0.08 < z' < 0.2$, with the upper portion, $z' > 0.2$, being the characteristic thermal plume region.

Another criterion for making comparisons between different fires is related to the heat transfer mechanism controlling the vaporization of fuel at the burning pool surface. Babrauskas [3], in a paper discussing the estimation of large pool fire burning rates, divides fires into 4 modes. The following table, which was excerpted from his paper, is based on the simplest assumptions. It relates the mechanism of heat transfer to the approximate size of the pool.

Diameter [m]	Burning Mode
< 0.05	laminar convection
0.05 - 0.2	turbulent convection
0.20 - 1.0	radiation, optically thin
> 1.0	radiation, optically thick

Thus when comparing features of fires which may be effected by the heat transfer mode, it is likely that the fires should be greater than one meter in diameter in order that this feature of large fires is duplicated.

The diffusion limited burning of hydrocarbon fuels results in the production of large amounts of soot. This soot strongly affects the radiative properties of the flame. Two effects are present:

- The soot causes the flame to be luminous, allowing radiation losses from the glowing soot to the ambient.
- In contrast to small luminous flames, optical paths are short compared to the flame thickness, thus energy from the center of the flame cannot easily escape.

Typical mean optical paths in these fires are near $1\ m^{-1}$ (Longenbaugh [4]). This implies that in a large fire, $D \gg 1$ m, much of the energy in the flame zone cannot be radiated out to the ambient. This leads to a situation, listed in the table above as "radiation, optically thick", in which the fuel surface can no longer see the ambient conditions. It also is expected that this will lead to higher temperatures. Thus, higher buoyancy forces prevail in the flame zone in these large fires in contrast to smaller luminous flames. This effect is difficult, if not impossible, to reproduce in smaller combustion experiments.

It should be noted that the optical thickness of the fire should be considered when examining thermocouple measurements in flames. In a small fire, the hot thermocouple radiates to the cool ambient. With large sooty fires, the thermocouple may not give the exact local temperature, but the error mentioned above is smaller because the thermocouple may only interact radiatively with hot combustion gases and soot within a few optical paths of it's location.

With the above information, it is clear that great care must be taken in extrapolating results for small fires to larger scales. The measurements of velocity and temperature made in the current study have been compared with the results of other measurements. Table 1 lists references in which velocity measurements have been made in low Froude number fires, of medium to

large area. The table lists the fuel type, pool size, estimated convective heat flux, heat flux per unit area, and value of Q^*. The measurements made in the current study were all within the continuous flame region, $z/Q^{2/5} < 0.08$, therefore, the range of vertical station locations is also listed in both dimensional and scaled forms.

The measurements of Cox and Chitty [5,6], and McCaffrey [2], were made with methane burner flames which are not highly luminous, however, the gas flow was very slow, giving values of Q^* comparable to large fires. The Raj paper [7] refers to experiments performed by NASA/White Sands. This work is also referenced as Johnson et al [8], and as Harsha et al [9]. Raj reports the velocity only at a single station above a JP-4 fire which lasts less than 4 minutes. Heskestad [10], has reported velocity measurements above a 0.29 m methanol fire. The only velocity measurements other than Raj made near pool fires greater than 1 meter in diameter were those of Kung and Stavrianidis [11]. This data was for various liquid fuels burning in pools ranging from 1.2 to 2.4 meters in diameter. Unfortunately, very few velocity measurements were made in the continuous flame zone in this work; most of the measurements are made in the intermittent region. Comparisons of these studies with the present results will be made in the results section of this paper.

Table 2 lists studies in which temperatures have been measured in large aviation fuel fires. The list is in order by pool surface area. The largest fires were the three huge tests by Yamaguchi and Wakasa [12] in which pool diameters range from 30 to 80 meters. Unfortunately, the results of these tests have only been made available in very sketchy form. Some studies have been left out of the table due to the presence of thermally massive test units in the fire near the thermocouples, and the possibility of these units causing changes in the thermal and flow fields near the point of measurement. All the fuels have similar heat release rates; so the value of burning rate has replaced the heat release rate in the table.

EXPERIMENTAL APPARATUS

This paper describes a test which was performed to evaluate a hazardous material shipping container. The test, performed February 26, 1986, involved the burning of approximately 48,500 liters of JP-4 fuel in a 9x18 meter pool. The test unit was 3.97 meters long by 2.44 meters wide by 2.74 meters in height, and was supported such that its' lower surface was 1.8 meters above the floor of the pool. In addition to measurements made within the test unit, measurements were made to help characterize the open pool fire environment. The discussion in this paper centers on these measurements. Figure 1 is a top view of the instrumentation in the pool. The instrumentation of primary interest involves the east tower and the plate calorimeter. A list of the instrumentation locations to be discussed is shown in Table 3.

A diagram of the location of measurement stations on the east tower is included as Figure 2. There were eight standard, ungrounded, 1.587 mm OD Inconel sheathed thermocouples protruding about 0.1 meter from the insulated, water cooled instrumentation tower at the locations listed in the figure. In order to make measurements of temperature with higher frequency response, smaller thermocouples were also used. Four bare junction thermocouples were used in this test. The thermocouples were type K, chromel-alumel, with a diameter of 127 μm. 20 gauge chromel and alumel wires were routed from the water cooled support tower to the measurement point through a 6.35 mm diameter ceramic rod 0.45 meter in length. The fine thermocouple wires were welded to the 20 gauge supporting wires, and butt welded together to form the measurement junction. Previous experience with this type of thermocouple indicates that mechanical failure occurs within minutes unless some protective measures are taken. In this case, a thin sol-gel glass coating (Brinker & Reed [19]) was applied to the fine wires which allowed measurements to be acquired over the entire 45 minute test. These thermocouples were placed at 0.152 meter intervals as is also indicated in Figure 2 and Table 3.

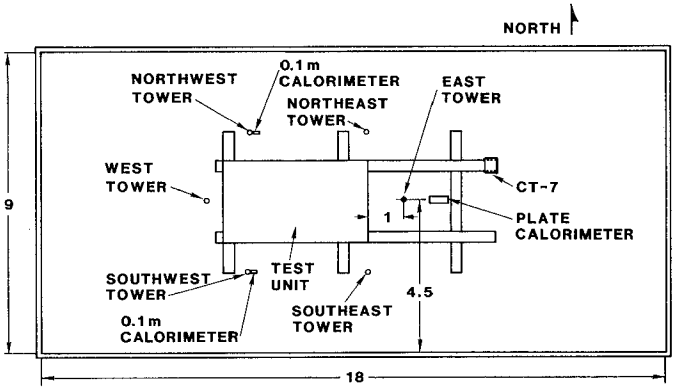

Figure 1. Open Pool Fire Test Facility
(Dimensions in meters)

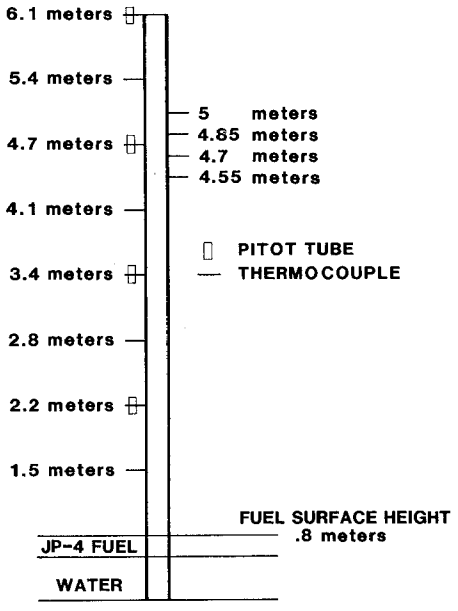

Figure 2. East Tower Instrumentation Scheme

The measurement of velocity above pool fires has been wrought with difficulties. Typical velocities are low, and the gas density is also low, thus the need for a very sensitive instrument exists. The fire environment is very harsh. The design of a sensitive probe which is durable has been problematic. A durable bidirectional, low-velocity probe, which is somewhat insensitive to changes in flow direction, was selected to measure the velocity in the fire plume. The design

is basically that of McCaffrey and Heskestad [20]. The only modifications were the addition of ruggedizing features, and a change in size. The probe is a device measuring, approximately, the difference between static and dynamic pressures, and using the Bernoulli relation to relate the measured pressure difference to fluid velocity.

$$W = \left[\frac{\Delta P}{\frac{1}{2} \rho C^2} \right]^{\frac{1}{2}} \qquad (2)$$

The four probes were manufactured from AISI 304 stainless steel. This material deteriorates under the conditions encountered in a large pool fire. In order to prevent deterioration, the probes were coated with sol-gel/glass powder film and the pressure sensing lines were water cooled and insulated. More specific details regarding the probe design and calibration can be found in Kent, et al. [21]. The probes were mounted on the 6 meter water cooled east tower as indicated in Figure 2. The sheathed thermocouples placed near each velocity probe measured the temperature of the gas near the probe. These temperatures were used in calculating the density of the fire products which in turn was used to calculate flame velocities. The pressure differences in inches of water were detected by electronic manometers (Airflow Developments Limited Model EDM 2500E).

Due east of the east tower on the long pool axis, a two sided mild steel panel calorimeter was mounted on an A-frame assembly. Each panel was 3.05 meters high by 0.61 meter wide. The bottom of the calorimeter was placed 2.13 meters above the pool floor. The south facing side was 6.35 mm thick, and the north side was 1.02 mm in thickness. The inside of this box was filled with insulation. The backface temperature measurements were made with intrinsic junction thermocouples at different heights along the centerlines of each of the two plates. Table 3 indicates the vertical placement of the measurement stations. An attempt to measure flame temperatures near the thicker south panel was also made. Sheathed thermocouples which protruded about 0.1 meter directly out from the centerline into the flames were installed at a number of vertical stations. Table 3, again, gives the exact placements.

The wind speed and direction were monitored with a propeller type anemometer located about 45 meters west of the pool at a height of about 3 m. A pressure transducer was used to record the fuel recession rate. This transducer was tapped into a 50 mm pipe that ran from the bottom of the west end of the pool to a sight glass located ≈45 meters away.

EXPERIMENTAL PROCEDURE

The ignition was performed at a single point in the northwest corner of the pool with an electric spark. Full engulfment of all instrumentation and the test unit occurred within 20 seconds. Data was gathered from the instrumentation using two systems. Temperatures from the thin plate calorimeter were measured with intrinsic thermocouples and logged on analog tape at a recording speed of 15 inches per second, with a Honeywell model 101 recorder. This data was digitized over 40 minutes of the fire at 40 samples per second and decimated down to 1000 data points. The same Honeywell tape recorder was used to record the signals from the bare wire thermocouples. In both cases it was necessary to amplify each thermocouple output with an Analog Devices thermocouple amplifier, AD595. The remaining data was acquired at six second intervals with an HP mini-computer and an HP 3497A data acquisition/control unit.

DATA REDUCTION AND UNCERTAINTIES

The signals from the thermocouples were converted to temperature using the standard type K curvefit equation. It should be noted that the flame temperatures reported here have not been corrected for radiation errors or compensated in any way. It is expected that when the thermocouple is surrounded by flames of depths greater than one meter, the errors due to radiation are small. There is concern when the thermocouple is not in a uniform temperature environment, but can see regions of widely varying temperatures. Thermocouples near the pool surface can see the pool, causing them to report temperatures lower than the actual local gas temperature.

Thermocouples near the test unit are affected by the presence of the test unit; errors of this type have been investigated by J. J. Gregory, et al. [22]. It should be noted that the test unit has a thin (~ 1 mm) stainless steel skin with insulation inside. Thus it is expected that the outer temperature responds fairly rapidly (within minutes) to the flame temperatures. Temperatures measured near the flame boundary, but in the ambient air, are expected to read high due to radiation coming from the flames. In this case, the errors are positive due to the low absorption of radiation by the ambient air. Typical time constants for the 1.58 mm diameter thermocouples used here range from 1 to 4 seconds depending on the local gas velocities and temperatures. Typical uncertainties in measured flame temperatures, considering only the thermocouples and measurement system, were ± 8°C.

The velocity probes were calibrated in a low speed wind tunnel for Reynolds numbers (based on probe diameter) from 300 to 3900, and tilt angles of 5 to 50 degrees. High uncertainties were present for Re_D less than 600. The probe Reynolds numbers, calculated from measured temperature and velocity histories, range from 700 to 2000. Thus all probes were operating in the range of low uncertainty. Typical uncertainty values for the calculated velocities, based on uncertainties in the pressure and temperature measurements, were estimated to be ± 0.7 meters/sec.

The density used in the calculation of velocity from the pressure difference is that of air at the measured temperature. This could lead to errors in the lower flame region where it is expected that significant fractions of unburned fuel vapor may be present. This factor was not included in the previous uncertainty estimate.

EXPERIMENTAL RESULTS AND DISCUSSION

Temperatures on Towers

The temperatures on the five towers were averaged over the test. This average was calculated from a start time, 20 seconds after ignition, to a final time near the end of the test, 2630 seconds after ignition. Figure 3 shows the average temperature versus distance from the pool floor for each of these towers. The standard deviations in temperature were also calculated and are plotted in Figure 4. At the higher stations, the wind more easily blows the flames away from the towers thus the variations in temperature become more pronounced.

Figure 5 shows a typical temperature history at a 6.1 meter station (east tower). The effects of wind on the temperature history are quite pronounced at this height. The low temperature dips were found to correspond to times when the tower tip was visible, uncovered by flame, and times which the wind measurements commonly indicated a strong component of wind blowing from the south. The probability density

function (pdf) of temperature measurements at the higher stations was examined, and found to be bimodal in shape. One mode at low temperatures corresponding with data taken when wind effects were strong, and the other mode at higher temperatures corresponding to the case when the instrumentation was fully covered with flame. The shape of the pdf's varied slightly from tower to tower, but all data including that taken from the small bare wire thermocouples showed a bimodal distribution of temperatures. A bimodal gaussian curve was fit to the sum of all pdf's from upper stations and the local minimum temperature was chosen as a setpoint temperature. In the current test this temperature was calculated to be 614 °C. Table 4 includes information about the bimodal curvefit coefficients calculated for thermocouple data mentioned above. A signal was generated from the temperature history at the 6.1 meter height for each tower, which was high when the temperature was above the setpoint, and low when the temperature was below the setpoint. This corresponds to a signal representing the "presence" or "absence" of flames at the 6.1 meter level. The correspondence is not exact; however, this is a simple starting place to help in examining the fire data with an attempt to account for the variability in wind effects.

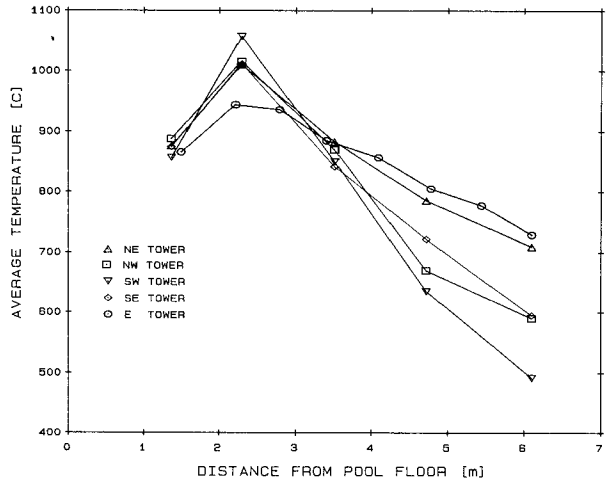

Figure 3. Average Flame Temperature (5 Towers)

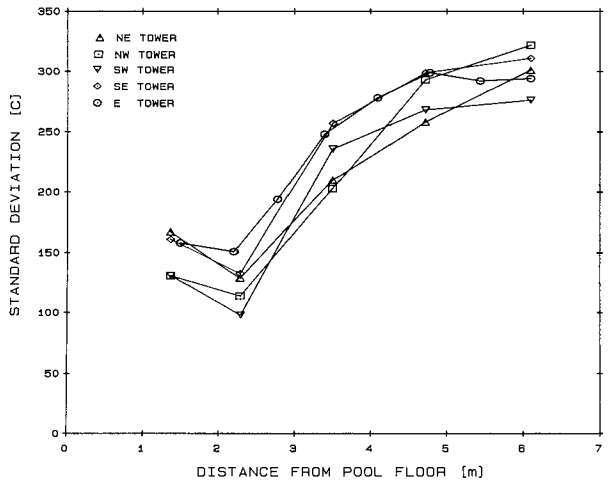

Figure 4. Standard Deviations in Temperature

Table 5 shows the correlation between thermocouples at various heights measured on the east, centrally located, tower. Temperatures along a tower were found to correlate quite strongly with each other near the top of the tower. The correlation degrades as the pool surface is approached. One interesting result is the reversal in correlation coefficient between the lowest and the upper stations. This implies that the wind which causes the temperatures at high stations to decline, is increasing temperatures near the pool surface. This negative correlation coefficient was found for data from all five tower locations.

Average temperatures were calculated for each thermocouple on the east tower based on data points taken when the "flame present at 6.1 meters" signal was high. Similar averages were calculated for the reverse condition. The averages for the other towers were calculated using the same procedures, the conditioning signal again generated for each tower from the temperature history at the top station. All of these averages are presented in Table 6. The averages during the times of low wind, which are the "flame present" averages, show a maximum temperature at approximately 4-5 meters above the pool floor, (3-4 meters above the fuel surface), and a significant decrease at the lowest stations. The maximum average temperature during flame present state is in a range from 950-1100 °C for all five towers. The flame absent averages look similar in shape to the averages with no conditioning, however the spread is smaller from tower to tower with the maximum difference being about 100°C at high stations.

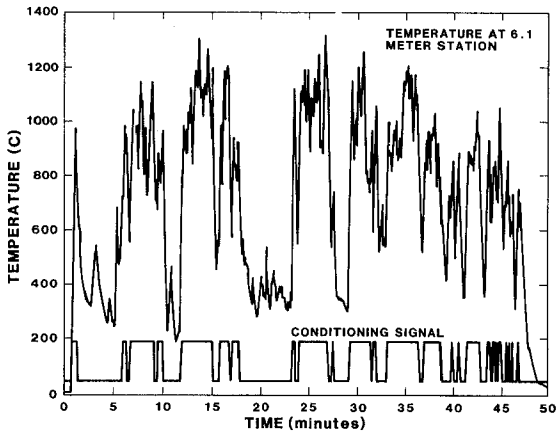

Figure 5. Temperature History at the 6.1 Meter Station and Conditioning Signal

Using the idea of conditioning allows the calculation of some other statistics which may reveal something about the nature of wind effects. The conditioning signal shown in Figure 5, can be described by two parameters: the fraction of time during the fire when the signal is high, and the typical frequency at which the signal flips back and forth. These two numbers were calculated for each of the five towers. The fraction of the time during which the flame is present will be defined as the flame intermittency. The intermittency gives some information as to the relative strength of wind effects on each tower. The typical durations of flame "presence/absence" lends some information about the time scales over which these wind effects act. This time scale data, it should be noted, may be strongly affected by the sampling rate and the time constant of the thermocouples used. The frequencies measured by looking at the intermittency signals here are likely to correspond to low frequency fluctuations in gross wind speed and direction. Table 7

lists the flame intermittency and typical flame duration times for each of the five towers. The strongest wind effects are present in the southwest corner of the pool, as was expected from the prevailing winds. The lowest wind effects, corresponding to the highest flame present fraction were found at the east tower. This condition is expected for a centrally situated tower that is less vulnerable to wind effects.

The bare wire thermocouple data was closely examined and two main conclusions were drawn. First, the temperatures reported by a bare wire thermocouple and a sheathed thermocouple near each other were very similar. This indicates that the local gas temperature must be fairly near the temperatures reported due to the difference in the radiative/convective partitioning between the two sizes of thermocouples. Secondly, it was observed that the flame present fluctuations were larger for the bare wire measurements than for standard sheathed thermocouples when both data sets were conditioned by the same signal (the conditioning signal derived from sheathed thermocouple data at the uppermost station). Table 8 shows the values of average and conditional average temperatures from the bare wire and sheathed thermocouple data. All the data presented in the table is for instrumentation located on the east tower.

Figure 6 compares the flame present data with results from the fires of Johnson, et al. [8], Bader [14], and Canfield and Russell [18]. In all of these investigations the averages are available over time periods when the wind effects are expected to be small, or the entire test took place in extremely mild wind conditions. In the case of Bader, it is expected that the use of thermally massive thermocouples also helped in reducing wind effects. Other studies listed in Table 2 which are not included in this comparison show clear effects of wind either in the test descriptions, or in the plots of flame temperature histories, and only report average values over the entire test. For examples, see Figure 3 in Gordon & McMillan [15], and Figure 3 in Tiger, et al. [13]. Hagglund mentions the presence of 4 m/s winds and "large temperature variations within the flames". In contrast, Russell [17,18] states that "temporal mean quantities are applicable only to the quasi-steady burning interval of the test flames as they exist in a quiescent atmosphere".

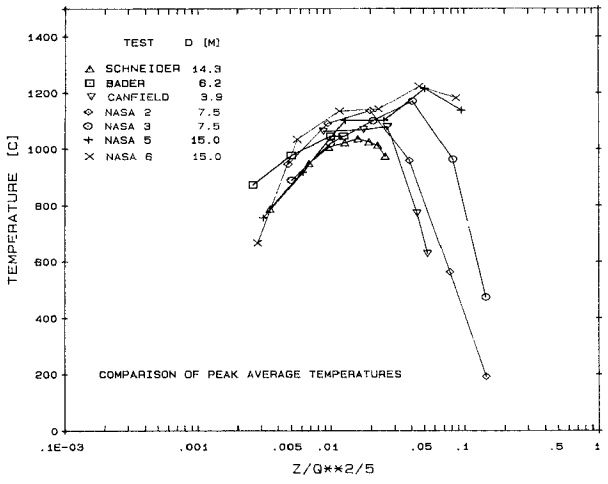

Figure 6. Temperature — Comparison with Literature

The data from Johnson is labeled "NASA #", where the # specifies his fire test number. An equivalent pool diameter is used in the figure for non-circular pools. That is the diameter of a round pool having the same surface area as the non-circular test pool. The actual pool shapes and sizes can be found in Table 2. The fires reported by Johnson showed strong decreases in temperature along the centerline compared with temperatures measured at slightly off center radial positions. These short tests were run under wind conditions of 0.08 m/s wind (tests 5 & 6), 0.22 m/s winds (test 3), and 0.44 m/s winds (test 2). The data plotted here is maximum average temperature reported at a given height. The low centerline temperatures were not observed in the present case and symmetry was not expected to be very good due to the presence of the test unit in the fire. It is expected that for these reasons the current data is more easily compared with maximum average temperatures. In general the curves agree in the lower continuous flame region and disagreement becomes quite pronounced as the intermittent flame region is approached. This is in part due to increasing sensitivity to differences in wind conditions in conjunction with averaging problems arising from the natural flame intermittency anticipated at these higher stations.

Gas Velocities on the East Tower

The velocity history for each probe station is shown in Figure 7. The large fluctuations in the velocities are primarily due to wind effects. Table 9 indicates the correlation between temperature and velocities measured at various vertical stations on the tower near the pool centerline. Note the strong correlation between velocity and temperature. It is not known how strong the correlation would be if only the flame present state was examined.

The velocity and temperature data was conditioned with the same signal. The average and conditioned average velocities are presented in Table 6. As previously mentioned the velocities during flame presence are significantly higher than those during flame absence.

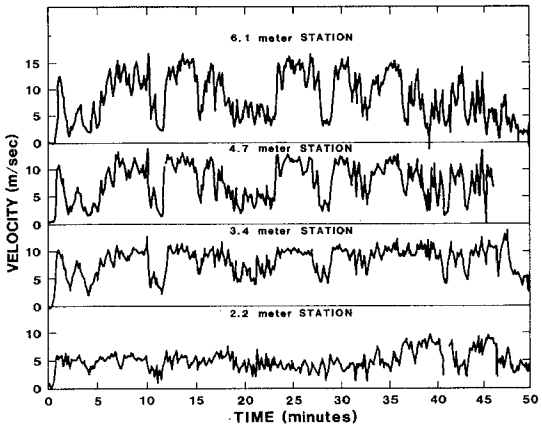

Figure 7. Velocity History at Each Station

Figure 8 compares the average measured velocities during the "flame present" state with the mean centerline velocity data for a number of much smaller fires. The vertical distance, z, has been scaled in a way which normalizes the flame height with the thermal

power of the fire. The data of McCaffrey [2] includes a large number of points with very little spread. In the figure, these points have been represented with a single line. The data of Cox and Chitty is in very good agreement with the data from McCaffrey. For this reason, only a single line is used. From a review of Table 1, it can be seen that the data of Kung and Stavrianidis is not in the same region of the flame as the current results; thus these data have not been included in Figure 8.

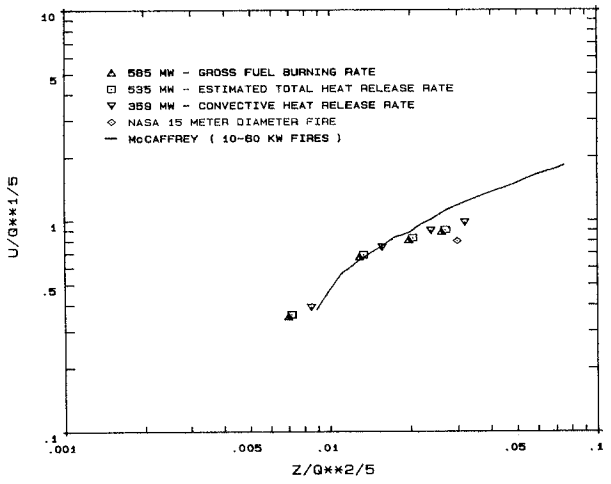

Figure 8. Velocity — Comparison with Literature

McCaffrey defines three zones in the fire: flame, intermittent flame and plume. The point $z/Q^{2/5} = 0.08$ is the end of the continuous flame region, $z/Q^{2/5} = 0.20$ is the end of the intermittent flame region. The vertical velocity was found to vary according to the relation of equation 3:

$$\frac{W}{Q^{1/5}} = 6.83 \left(\frac{z}{Q^{2/5}} \right)^{1/2} \qquad (3)$$

in the continuous flame region. The value of Q used in equation 3 by McCaffrey was the estimated total heat release. In McCaffrey's work, the flames studied were methane flames which were not highly luminous. In this case the theoretical maximum heat release (from gross fuel consumption), the estimated total heat release (considering combustion efficiency), and the convective heat release, were very near the same values for a given flame. In the case of a sooty pool fire these values will differ considerably from each other. It is likely that only the convective heat released contributes to the buoyancy, and thus to vertical velocities. Due to the lack of velocity data from sooty pool fires, velocities for all three heat release rates are plotted in Figure 8. The single data point from the NASA fire, which was reported in the paper by Raj, has also been included in Figure 8.

Exterior Temperatures on the Plate Calorimeter

Nine thermocouples were placed with a 0.305 meter vertical spacing on the south (6.35 mm thickness) side of the large plate calorimeter. The thermocouples protruded 0.1 meter from the plate into the flames. The average temperature over the time of the fire was calculated from the temperature histories for these thermocouples. Conditional sampling similar to that used with the tower thermocouples was used to calculate conditional averages. The conditional signal was generated from the uppermost temperature. When this temperature was above the setpoint value, the flame present condition was assumed. Averages for each of the nine thermocouples were calculated using this conditioning signal generated from the top station. These averages are listed along with the average temperatures over the entire test in Table 10.

The flame absent average temperatures, external to the plate, follow the flame absent average tower temperatures in Table 6 very closely. The flame present and entire test average temperature curves show the same general trends as have been described for the tower data, however the values are ≈40°C higher. This may be due to some attenuation of the wind effects by the presence of the nearby plate.

The average fire temperature during the flame present state was relatively constant with height, with a value of ~1065°C. The temperature histories of these thermocouples, though not included here, look very similar to the east tower temperature histories.

Results from the Thick Plate Calorimeter

The steel backface temperature data for the 2 stations on the 6.35 mm thick panel calorimeter are presented in Figure 9 along with 2 backface temperatures from the thin (1.02 mm thickness) walled calorimeter. The maximum thick wall backface temperature at any given time was at the lowest, 2.5 meter, station with the temperature decreasing with elevation. The maximum temperature difference between the 2.5 and 5 meter stations was 330°C.

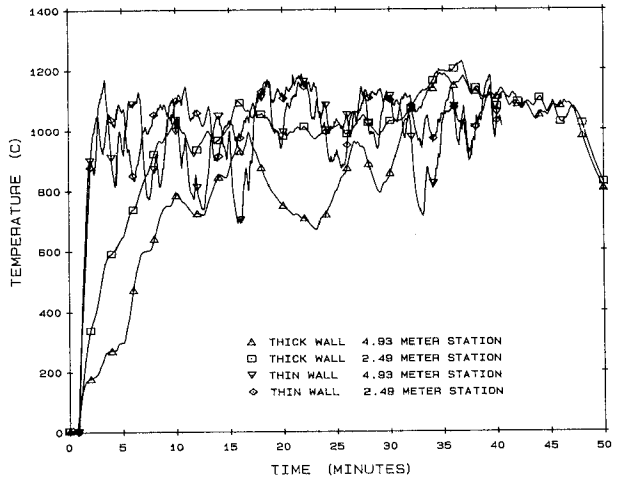

Figure 9. Calorimeter Backface Temperature Histories

Figure 10 shows a plot of typical results obtained from the thick walled calorimeter. The plot indicates the flame and plate temperatures which were measured at the uppermost, 4.93 meter, station. The Sandia One Dimensional Direct and Inverse Thermal Code, (SODDIT), was employed to estimate the plate surface temperatures and heat fluxes using only the plate backface temperature history, and the calorimeter material properties. The details of the code can be found in Blackwell, et al. [23], and more general theoretical considerations are referred to Beck, et al. [24]. The calculated surface temperature was near enough to the backface temperature at all times that plotting the two on the scale of Figure 10 would show no difference. Thus the plate temperature has been characterized in the figure as a single line labeled "plate temperature".

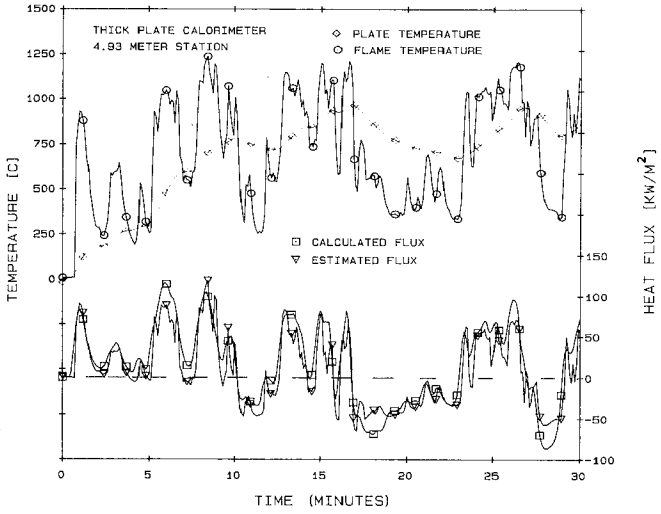

Figure 10. Heat Fluxes and Temperatures for Thick Plate Calorimeter

The calculated heat flux has also been plotted in the figure and is labeled as "Heat Flux Calculated". The assumption was made that the external thermocouple measurements were reasonably accurate representations of the flame temperatures and a simple model was used to estimate the expected flux given the surface and flame temperature histories. A simple equation for Q is:

$$Q_{est} = \sigma \epsilon (T_f^4 - T_s^4) + h (T_f - T_s) \qquad (4)$$

An estimate of h and ϵ were made utilizing a non-linear parameter estimation routine. The values of ϵ and h were assumed constant over the duration of the fire. For the case shown in the figure the values of h and ϵ found which minimize the least squares difference between the estimated Q and the calculated Q were:

$$\epsilon = .462 \qquad h = 39.11 \ \frac{W}{m^2\ °K}$$

The heat flux calculated using equation 4 and the above constants is shown in the Figure labeled "Estimated Flux". Note that the fit between the flux calculated by the inverse code and the flux estimated by equation 4 is fairly good. The partitioning of the heat flux between radiation and convection using the above assumptions will depend on the flame and surface temperatures; for a flame temperature of 1100°C and a surface temperature of 540°C this gives a radiant Q of 86 kW/m² and a convective Q of 22 kW/m². Thus, in this example the radiative fraction is about 80% of the total flux.

The heat flux histories for all the stations on the panel were calculated using the inverse code. From these histories and some simplistic assumptions about the mechanism of heat transfer, flame temperatures may be estimated. Peak fluxes to the calorimeter ranged from 80 - 120 kW/m². The effective flame temperatures for blackbody fluxes ranged from 815 - 930 °C. The theoretical convective/radiative partitioning for a flat plate was also estimated. The average convective contribution to the flux at a surface temperature of 150 °C would be ~5% for the entire length of the plate. For a given flame temperature, the convective flux would be higher at the lower stations and would decrease with height. Initially, the fluxes were highest at the lowest elevation and decreased with increasing elevation. This trend, however, reversed as the test continued.

The flame temperatures at the 2.5 meter station were, in general, higher and more uniform than the temperatures at the 5 meter station. The fluctuating nature of the fire that is seen for the flame temperature data is also exhibited in the heat flux to the plate. The large amplitude oscillations in flame temperature at the upper stations create oscillations in the heat flux that are larger in amplitude than those experienced at the lower stations.

Thin Plate Calorimeter

Temperatures were measured at 4 stations on the insulated backface of the thin walled (1.02 mm thickness) north side, of the large plate calorimeter. The stations are located at elevations which range from 2.5 meters to 5 meters above the pool floor.

The average values and standard deviations of the plate temperatures were calculated over the entire test ignoring the first 100 seconds of heat up data. These results are included in Table 10. The average temperature of the plate was higher than any flame temperature averages. It is expected that this is in part due to the fact that the plate faced north, and the prevailing winds were from the south or southwest. The standard deviation in the plate temperature was about half the standard deviation in flame temperatures at corresponding heights from the pool. This is due to the damping of thermal fluctuations by the plates' thermal mass.

Fuel Levels and Burn Rate

The fuel recession rate in this type of test is usually found in two ways. An average rate can be determined simply by dividing the total fuel consumed by the duration time of the test. Secondly, a pressure transducer can be used to determine the variation in recession rate during the test by recording the pressure in the pool. In this test a leak in the fuel delivery system caused some problems in the interpretation of the pressure transducer results, however the average burning rate could still be determined with good accuracy by the first method.

Initially, 0.61 meters of water was brought into the pool. In the 9.1 meter by 18.3 meter pool, a one millimeter height of liquid is 167 liters. 34,000 liters of fuel was then added to achieve a total burn time of approximately 30 minutes. This increased the total liquid level to 0.814 meters. This was verified by a tape measure located inside the pool. During the test, a leak in the fuel delivery system introduced additional fuel into the pool, thereby increasing the burn time to 46 minutes. A total of 48,460 ± 380 liters of fuel was brought into the pool. The average fuel recession rate was therefore calculated to be 6.29 ± 0.06 mm of fuel per minute. This is very consistent with previous burning rates in this pool.

Wind Speed Measurements

Figure 11 is a plot of the magnitude and components of the wind speed during the time of the test. On this plot ignition occurred at approximately 50 seconds, and the fire was out at a time of about 46 to 47 minutes. The mean wind speed over the time of the burn was 1.68 meters per second. The standard deviation from the mean value was 0.95 meters per second. The wind speed was seen to increase as the test progressed with the maximum value of 4.2 meters

per second occurring ~ 37 minutes into the test. The velocity components of the wind in the east/west, and the north/south directions were also computed and examined exhaustively for any connection with the intermittency. Though some correlation exists, it is expected that the fire influenced the flow field around it. The wind measurements needed to anticipate the flame's shape are much more extensive than those gathered in these tests.

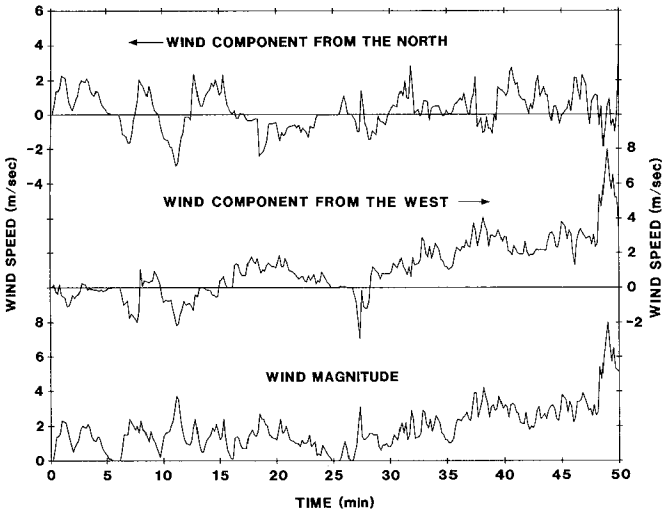

Figure 11. Wind Speed and Direction During Test

CONCLUSIONS

The measurements of gas velocity made in the lower continuous flame region in this study agree well with the data available from smaller fires. Velocity measurements at higher stations than those addressed here, (in the upper continuous flame and the intermittent flame region), in fires of this size have not been published to date. These measurements should be attempted to see if the agreement with small fires continues in this region.

Temperatures measured in this study have been compared with the results of others. Comparisons are difficult to make due to the lack of information in many cases about the existing winds, and the known strong wind effects. In spite of these difficulties, a scheme has been attempted which mitigates, to some degree, the effects of mild wind conditions. The average temperatures conditioned for times of low wind have been compared with results of other workers taken during times of "quasi-steady" burning and reasonable agreement was found at low stations ($z/Q^{2/5} < 0.02$).

The measurements of heat flux to a large vertical plate was reported. Some simple attempts at estimating the flux from measured surface and flame temperatures are also included.

ACKNOWLEDGEMENTS

The authors would like to acknowledge the effort and significant contributions of all those who participated in the planning and execution of this test. Our appreciation is extended to Ned Keltner, Julie Gregory, Bob Mata, Dan Luna, Bill Jacoby, and to any and all technical, millwright, and labor support whose work was instrumental in the performance of this test.

REFERENCES

1. Zukoski, E.E., "Fluid Dynamic Aspects of Room Fires", Proceedings of the First International Symposium on Fire Safety Science, pp. 1-30, 1986.
2. McCaffrey, B.J., "Purely Buoyant Diffusion Flames: Some Experimental Results," NBSIR 79-1910, National Bureau of Standards, 1979.
3. Babrauskas, V., "Estimating Large Pool Fire Burning Rates," *Fire Technology*, **19**, No. 4, pp 251-261, 1983.
4. Longenbaugh, R.S., "Experimental and Theoretical Analysis of the Radiative Transfer Inside of a Sooty Pool Fire," M.S. Thesis, New Mexico State University, 1985.
5. Cox, G., and Chitty, R., "A Study of the Deterministic Properties of Unbounded Fire Plumes," *Combustion and Flame*, **39**, pp. 191-209.
6. Cox, G., and Chitty, R., "Some Source Dependent Effects of Unbounded Fires," *Combustion and Flame*, Vol. **60**, pp. 219-232.
7. Raj, P.K., "Analysis of JP-4 Fire Test Data and Development of a Simple Fire Model," ASME Paper Number 81-HT-17.
8. Johnson, H.T., Linley, L.J., and Mansfield, J.A., "Measurement of the Spacial Dependence of Temperature and Gas and Soot Concentrations Within Large Open Hydrocarbon Fuel Fires," NASA Technical Memorandum 58230, 1980.
9. Harsha, P.T., Bragg, W.N., and Edelman, R.B., "A Mathematical Model of a Large Open Fire," Science Applications Inc., NASA Contract Report # NAS2-10675. also NASA #SAI-81-026-CP
10. Heskestad, G., "Peak Gas Velocities and Flame Heights of Buoyancy-Controlled Turbulent Diffusion Flames," *Eighteenth Symposium (International) on Combustion*, pp. 951-959, The Combustion Institute.
11. Kung, H.C., and Stavrianidis, P., "Buoyant Plumes of Large-Scale Pool Fires," *Nineteenth Symposium (International) on Combustion*, pp 905-912, The Combustion Institute.
12. Yamaguchi, T., and Wakasa, K., "Oil Pool Fire Experiment," Proceedings of the First International Symposium on Fire Safety Science, pp. 911-918.
13. Alger, R.S., Corlett, R.C., Gordon, A.S., and Williams, F.A., "Some Aspects of Structures of Turbulent Pool Fires," *Fire Technology*, **15**, pp. 142-156.
14. Bader, B.E., "Heat Transfer in Liquid Hydrocarbon Fuel Fires", *Chemical Engineering Progress Symposium Series*, Vol. 61, No. 56, pp. 78-90, 1965.
15. Gordon, W., and McMillan, R.D., "Temperature Distribution within Aircraft-Fuel Fires," *Fire Technology*, Feb. 1965, pp. 52-61.
16. Hagglund, B., "The heat radiation from Petroleum Fires," FoU-brand, pp. 18-24, 1977.
17. Russell, L.H., "Quantification of the Heat Transfer Parameters Relevant to a Cylinder Immersed in a Large Aviation Fuel Fire," M.S.M.E. Thesis, University of Pittsburgh, 1970.
18. Russell, L.H., and Canfield, J.A., "Experimental Measurement of Heat Transfer to a Cylinder Immersed in a Large Aviation-Fuel Fire", *J. Heat Transfer*, **95**, p. 397, 1973.
19. Brinker, C.J., Reed, S.T., "Low Temperature Process for Obtaining Thin Glass Films", Sandia National Laboratories, Patent No. 4476156, October, 1984, Albuquerque, New Mexico.
20. McCaffrey, B.J., and Heskestad, G., "A Robust Bidirectional Low-Velocity Probe for Flame and Fire Application", *Combustion and Flame*, **26**, pp. 125-127, 1974.

21. Kent, L.A., and Schneider, M.E., "The Design and Application of Bi-directional Velocity Probes for Measurements in Large Pool Fires," ISA Symposium, Las Vegas, NV, 1987.
22. Gregory, J.J., Mata, R. Jr., Keltner, N.R., "Thermal Measurements in a Series of Large Pool Fires", SAND 85-0196, Sandia National Laboratories, Albuquerque, New Mexico, 1987.
23. Blackwell, B.F., Douglas, R.W., "A Users Manual for the Sandia One-Dimensional Direct and Inverse Thermal Code", SAND85-2478, Sandia National Laboratories, Albuquerque, New Mexico, 1986.
24. Beck, J.V., Blackwell, B.F., St. Clair, C.R. Jr., Inverse Heat Conduction, John Wiley & Sons, 1985.
25. McCaffrey, B.J., "Momentum Implications for Buoyant Diffusion Flames," *Combustion and Flame*, 52, pp. 149-167.

Table 1 - Velocity Measurements in Low Froude Number Fires.

Author	Fuel	Pool Diameter [m]	Measurement Height [m]	Estimated Q_c [kW]	z/Q_c^{*4} [m/kW$^{.4}$]	Q_c/A [kW/m^2]	Q^*
Kung & Stavrianidis [11]	Heptane	1.219	1.26 - 8.88	2180	0.057 - 0.40	1870	1.2
	Heptane	1.737	1.26 - 8.88	4367	0.044 - 0.31	1840	1.0
	Methanol	2.438	1.26 - 8.88	1498	0.067 - 0.47	321	0.15
	Hydrocarbon F1	1.737	1.26 - 8.88	1546	0.067 - 0.47	652	0.35
Raj [7]	JP-4	15.24	5.73	348000	0.0348	1910	0.35
Cox & Chitty [5] & [6]	Methane	0.3 (square)	?	14 - 47	0.030 - 0.4	160 - 520	0.3 - 0.9
	Methane	0.45 (square)	?	45 - 120	?		
	Methane	0.60 (square)	?	45 - 120	?	127 - 327	0.13 - 0.28
McCaffrey [2]	Methane	0.30 (square)	.10 - 1.5	14.4 - 57.5	0.009 - 0.50	160 - 640	0.3
Heskestad [10]	Methanol	.29 (square)	?	30.77	?	366	0.45
Current	JP-4	9 x 18 (rect)	1.4 - 5.3	359000	0.0084 - 0.032	2216	0.42

$Q_c/Q_{theory} \approx 0.61$

Table 2 - Temperature Measurements in Aviation Fuel Fires.

Author	Fuel	Pool Diameter [m]	Measurement Height [m]	Burning Rate [mm/min]
Canfield & Russell [17]	JP-5	2.4 x 4.9 (rec)	.6,1.2,1.8,3.0,3.6	?
Alger [13] et. al.	JP-5	3.05	.01,.40,1.2	5.78±1.55
Johnson et. al [8]	JP-4	7.5	0.7,1.4,2.9,5.7,21.3	?
	JP-4	15.24	0.7,1.4,2.9,5.7,21.3	5.3
Bader [14]	JP-4	5.5 (square)	0.2,0.4,0.56,0.76,1.0,1.27	?
Gordon & McMillan [15]	JP-4 AvGas JP-5	3.6 x 7.3 (rec)	0.152 - 1.67	
Yamaguchi & Wakasa [12]	Kerosene	30,50,80	?	4.7
Hagglund[16]	JP-4	.5 - 10 (sq)	?	≈ 4.0
Current	JP-4	9 x 18 (rect)	1.4 - 5.3	6.29

Table 3 - Instrumentation Locations

Instrumentation	Vertical Distance from pool floor [m]
East tower - 1.59 mm OD Thermocouples	1.5, 2.21, 2.79, 3.4, 4.09, 4.78, 5.44, 6.1
East tower - 0.13 mm OD Thermocouples	4.55, 4.7, 4.85, 5.0
East tower - 25.4 mm OD Velocity probes	2.21, 3.4, 4.78, 6.1
TCs on insulated backface of Thick wall	On 0.30 centers from 2.44-4.84
TCs on insulated backface of Thin wall	On 0.81 centers from 2.44-4.88
TCs external to Thick Wall	On 0.30 centers from 2.44-4.84
Northeast tower thermocouples	1.37, 2.29, 3.51, 4.72, 6.1
Northwest tower thermocouples	1.37, 2.29, 3.51, 4.72, 6.1
Southeast tower thermocouples	1.37, 2.29, 3.51, 4.72, 6.1
Southwest tower thermocouples	1.37, 2.29, 3.51, 4.72, 6.1
Initial Fuel Level	0.81

Table 4 - Table of Bimodal Fit Coefficients

A probability density function of temperature was constructed from all temperatures measured at the 6.1 meter station from all 5 poles during the time of the fire. A curve was fit to the pdf of the form :

$$Y = a_1 e^{-\frac{1}{2}\left(\frac{T - T_{off1}}{\sigma_{t1}}\right)^2} + a_2 e^{-\frac{1}{2}\left(\frac{T - T_{off2}}{\sigma_{t2}}\right)^2}$$

Where Y is the number of temperatures measured within 7 °C of the temperature T. The values of the constants were found to be :

$a_1 = 29 \pm 1.62$ $\quad a_2 = 16 \pm 1.07$

$\sigma_{t1} = 112 \pm 8$ °C $\quad \sigma_{t2} = 252 \pm 28$ °C

$T_{off1} = 349 \pm 7.9$ °C $\quad T_{off2} = 911 \pm 22.5$ °C

Table 5 - Correlation between Temperatures on the East Tower

	Vertical Stations [meters]							
	6.10	5.44	4.78	4.09	3.40	2.79	2.21	1.50
6.10	1.00							
5.44	.98	1.00						
4.78	.91	.97	1.00					
4.09	.83	.90	.97	1.00				
3.40	.73	.80	.90	.95	1.00			
2.79	.52	.58	.69	.78	.92	1.00		
2.21	.15	.22	.34	.47	.67	.88	1.00	
1.50	-.53	-.54	-.49	-.39	-.19	.15	.52	1.00

Table 6 - Average Temperatures and Velocities

	Height [m]	Average	Std Dev	Flame Present	Flame Absent
Velocity [m/s]	6.10	9.5	4.1	12.6	6.0
	4.78	8.9	3.4	11.6	6.0
	3.40	8.2	2.2	9.6	6.6
	2.21	4.8	1.7	5.0	4.6
East Tower Temperatures [°C]	6.10	729	294	932	408
	5.44	777	292	979	457
	4.78	805	299	1000	496
	4.09	857	278	1020	598
	3.40	885	248	1012	684
	2.79	936	194	1004	828
	2.21	944	151	957	924
	1.50	866	158	798	975
SW Tower	6.10	492	276	959	369
	4.72	635	268	1034	530
	3.51	850	236	1131	776
	2.29	1057	98	1059	1057
	1.37	857	131	751	885
NW Tower	6.10	590	322	918	349
	4.72	670	293	969	450
	3.51	870	203	1046	740
	2.29	1016	114	1026	1008
	1.37	888	131	793	958
NE Tower	6.10	709	301	935	407
	4.72	785	258	954	558
	3.51	883	210	975	760
	2.29	1010	129	979	1051
	1.37	876	167	788	993
SE Tower	6.10	595	311	933	365
	4.72	722	299	1024	517
	3.51	842	257	1050	700
	2.29	1012	133	978	1035
	1.37	875	161	752	959

Table 7 - Flame Intermittency and Wind Frequencies

Tower	Flame Intermittency	Typical Time of Flame Presence [s]
SW	20.8 %	598
SE	40.5 %	414
E	61.3 %	270
NE	57.2 %	358
NW	42.4 %	538

Table 8 - Bare Wire Thermocouple Comparison

	Bare Wire (127 μm)	Sheathed TC
Height from pool floor	4.70 m	4.78 m
Average temperature	721.7 °C	786.7 °C
Standard Deviation	323.9 °C	310.5 °C
Flame present average	887.1 °C	1005.0 °C
F.P. Std. Deviation	256.9 °C	163.3 °C

Intermittency = 0.613; Averaged from 50-2750 Seconds;
Both signals subject to conditioning signal generated from 6.1 meter station sheathed thermocouple data.

Table 9 - Correlations with Velocities

	Velocity probe locations [meters]			
	6.10	4.78	3.40	2.21
Tower Temps [meters]				
6.10	.86	.89	.77	.13
5.44	.81	.89	.83	.24
4.78	.70	.82	.85	.33
4.09	.61	.75	.84	.37
3.40	.53	.66	.79	.33
2.79	.38	.47	.62	.24
2.21	.07	.14	.35	.21
1.50	-.38	-.48	-.43	-.24
Velocities [meters]				
6.10	1.00			
4.78	.93	1.00		
3.40	.68	.85	1.00	
2.21	-.05	.18	.53	1.00

Table 10 - Average Temperatures from plate calorimeter

Measurement	Height From Floor [Meters]	Average [°C]	Std. Dev. [°C]	Flame Present [°C]	Flame Absent [°C]
Temperatures External to Plate	4.93	846	303.1	1006	675
	4.62	855	294.3	1009	689
	4.31	886	275.3	1030	731
	4.01	902	262.1	1039	756
	3.71	920	242.9	1044	786
	3.40	942	221.8	1052	825
	3.10	964	198.1	1057	865
	2.79	984	174.4	1058	906
	2.49	1003	149.3	1050	953
Thin Plate Backface Temperatures	4.93	985	116.7		
	4.11	1015	109.1		
	3.30	1102	98.3		
	2.49	1044	74.9		